Journal of Asian Concrete Federation
Vol. 2, No. 1, pp. 1-14, June 2016
ISSN 2465-7964 / eISSN 2465-7972
http://dx.doi.org/10.18702/acf.2016.06.2.1.1

Mesoscale study of water transport in mortar influenced by sodium chloride

Yi Wang, Fuyuan Gong, Dawei Zhang* and Tamon Ueda

(Received: February 1, 2016; Accepted: May 16, 2016; Published online: July 05, 2016)

Abstract: Transport properties of mortar exposed to salt solution are fundamental information for understanding the durability of mortar. In this paper, change in moisture uptake behaviors due to sodium chloride (NaCl) contamination was studied. To understand the salt contamination effect, mortar samples with different water-to-cement ratios (*w*/*c*) in meso scale were immersed into deionized (DI) water, intermediate (3%wt), and high (20%wt) concentration of NaCl solutions for three days. After immersion, the re-dried samples were sequentially immersed in DI water at room temperature for seven days. Based on the test results, two-stage solution diffusion model was developed, which can describe the solution absorption process efficiently. The salt contamination may be due to calcium (Ca^{2+}) leaching and salt crystallization. As found, when exposed to low concentration NaCl solution, the diffusivity of mortar would increase due to faster Ca^{2+} leaching. However, for high concentration NaCl solution, it would be reduced since pores filled by crystallized salt have dominant effect in this case. The salt crystallization mainly occurs at small pores because there is little difference at initial absorption but the difference becomes significant for long time absorption.

Keywords: absorption, sodium chloride solution, salt crystallization, sorptivity, mortar.

1. Introduction

In cold and wet regions, frost damage of concrete is an important durability issue to concern, especially for the concrete structures exposed to deicing agents in winter [1]. In order to predict the service life of concrete structures exposed to frost action, water transport properties were used as an index [2]. However, when the concrete is contaminated by the deicing salt, the transport properties of concrete would be very different with the one exposed to frost action only [3, 4]. Thus, the transport properties of concrete exposed to deicing agent need further investigation [5].

When the chloride ion penetrates into concrete, on one hand, it binds to cement pastes by chemical reactions (salt crystallization) and physical adsorption [6,7]. The salt crystallization increases solids volume because the formation of Friedel's salt filling the voids may induce expansion [8] and consequently alters the pores diameter of mortar [9]. On the other hand, when the concrete is exposed to salt solution, calcium hydroxide in concrete may dissolve into solution and leach out. In particular, with the presence of sodium chloride (NaCl), the process of calcium (Ca^{2+}) leaching may be accelerated and the porosity will increase correspondingly [10]. Since the rate of liquid absorption is related to the diameter of each pore [11-13], if the pore diameter changed due to the salt crystallization or Ca^{2+} leaching, the solution transport will be affected. Therefore, by analyzing the liquid absorption, the salt effect on pore characteristics of concrete may be clarified.

Researchers have studied the liquid absorption for decades because it is an important parameter for durability of concrete [14,15]. Since the liquid absorption test was mainly conducted in macro scale [16,17], for the salt solution absorption, the pore solution concentration may vary from surface to depth of concrete [18], which makes the salt crystallization effect on transport properties difficult to understand. So the specimen in small size is a good option for this study, but there are few studies concerning on the small scale. Although Macinnis and Nathawad [19] developed meso-scale solution absorption testing method, their purpose

Corresponding author Dawei Zhang is an Associate Professor of the College of Civil Engineering and Architecture, Zhejiang University, China.
Yi Wang is a Ph.D. Student, Graduate School of Engineering, Hokkaido University, Sapporo, Japan.
Fuyuan Gong is a Post Doctoral Researcher of Concrete Laboratory, Department of Civil Engineering, The University of Tokyo, Tokyo, Japan.
Tamon Ueda is a Professor, Faculty of Engineering, Hokkaido University, Sapporo, Japan.

was to measure the absorptivity and permeability of concrete. The absorption process difference with different concentration NaCl solutions was described, however, how the micro characteristics had been changed with different NaCl solutions and how the Ca^{2+} leaching and salt crystallization would affect transport properties of concrete were still not clarified.

In this paper, the main purpose is to understand how the combined salt crystallization and Ca^{2+} leaching alter the pore characteristics of mortar with different concentrations of NaCl solutions and then influence the water transport. Since the coarse aggregate has rather low permeability, the transport properties of concrete are mainly determined by mortar. The experimentation was conducted in meso-scale. In the meso-scale, which is in the order of five millimeters, the pore solution concentration in mortar could be considered as uniform [1], thus the salt effect can be analyzed by comparing the results of absorption of NaCl solutions and reabsorption of deionized (DI) water. Based on the solution properties analysis and the proposed liquid transport model, the effect of salt crystallization and Ca^{2+} leaching to pore characteristics of mortar can be analyzed separately. The analyzed results such as relative absorbed water, matrix mass change, and diffusivity change are discussed in detail in this paper.

2. Test programs

To understand the pore characteristics and transport properties change due to combined Ca^{2+} leaching and salt crystallization, the absorption test was adopted in this study by applying gravimetry. The microstructural alterations due to Friedel's salt formation and calcium leaching were observed through SEM images by Liu et al. [9]. In their study, immersed in DI water, the pore size of concrete increased due to calcium leaching, while it decreased with 5% (by wt.) NaCl solution because of formation of Friedel's salt. The research has qualitatively provided the information of microstructural alterations due to NaCl existence, and their results are consistent with our findings. Therefore, the SEM observation was not carried out in this study.

2.1 Specimen and solution preparation

Mortar specimens were used in this experimental program. The materials used were ordinary Portland cement with density of 3.16 g/cm^3 and fine aggregate which is 1.2 mm or less in size with density of 2.67 g/cm^3 without air entraining agent. Mix proportions are based on ACI 211.1 [20], as shown in Table 1 with different water-to-cement ratios (*w*/*c*). The materials were mixed properly, and then cast into 40×40×160 mm form and cured for 24 hours prior to removing the form. Once demolded, specimens were cured under water for 90 days at the temperature of 20 to 23°C. After curing, specimens were cut into meso-scale size of 70×30×5 mm for absorption test. As can be seen in Fig. 1(d), the surface of mortar was removed and the core part was used for test. In this case, the property of samples can be assumed uniform. The details of preparation of specimens can be seen in Fig. 1. To obtain dry condition, specimens were put inside of oven for 24 hours at 105°C to remove evaporable water. After drying, they were sealed with saran carefully to prevent moisture transfer until measuring their weight under normal temperature and vacuumed chamber was used to store the dried specimens for test.

In order to get fully resolved solutions, the NaCl solute was stirred properly with deionized water in plastic container with volume of 4 liters. Sodium chloride solutions of 0, 3%, and 20% by mass concentration were prepared 24 hours before testing.

The density and porosity of mortar were measured gravimetrically by immersing samples into DI water. First of all, the samples were dried by oven at 105°C and the mass was measured at normal temperature. Then the samples and DI water were put into vacuum desiccator separately for 15 minutes to remove the air inside of samples and DI water. After that, the samples were immersed into the DI water in a container. They were continuously staying in the vacuum desiccator for one hour until they were moved out, sealed and placed at room temperature of 20 to 23°C. After immersing for 7 days, it was assumed that the samples were fully saturated and then mass was measured. The apparent volume of samples was obtained by suspending the sample into DI water. When the samples are suspended in the water, the measured mass change of water container (before and after immersion of the sample in the water) is equal to the mass of water flow away and this amount of water volume is the same as apparent volume of sample (apparent volume means including the pore inside since they were filled with water beforehand). Finally, the porosity and bulk dry density of samples were calculated based on the measured mass and volumes. Skeletal density was also calculated with porosity and bulk dry density subsequently. The results are presented in Table 1. The test performed and number of specimens is summarized in Table 2.

Table 1 – Mix proportions and properties of mortar

Water/cement Ratio (w/c)	Water kg/m^3	Cement kg/m^3	Fine aggregate kg/m^3	Bulk dry density (ρ_b) kg/m^3	Skeletal density (ρ_0) kg/m^3	Porosity
0.3	207	690	755	2,173	2,676	0.188
0.5	207	414	990	2,137	2,688	0.205
0.7	207	296	1,090	2,125	2,703	0.214

Table 2 – Summary of test performed and numbers of specimens

Test performed	Absorption test			Porosity
	DI water	3% NaCl	20% NaCl	
w/c=0.3	3	3	3	3
w/c=0.5	3	3	3	3
w/c=0.7	3	3	3	3

(a) sieving the sand (1.2mm or less)

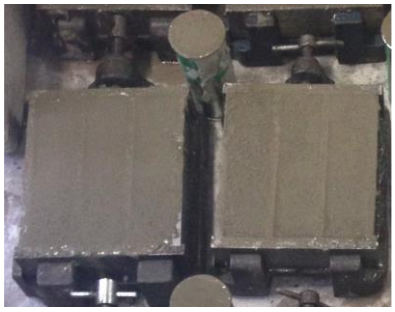

(b) casting the mortar

(c) curing under water

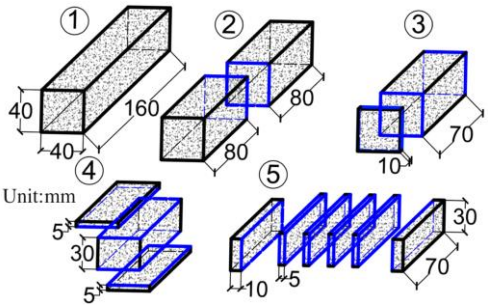

(d) cutting procedures

(e) cut specimens 70×30×5 mm

Fig. 1 – Preparation of specimens

2.2 Absorption test procedures

Firstly, the dried weights of specimens were measured with a scale while the accuracy was 0.1 mg. During the first one minute, the specimen was grasped by a tweezer. By doing so the specimen could be fixed to a certain place and easily taken out from solution. As a result, the time of specimen immersed in solutions can be exact as designed (see Fig. 2(a)). The first minute is highlighted because the immersion time at the initial stage is very sensitive to the absorption results. Based on the understanding of solution absorption [21], the interval time of measurement is not constant, but increasing with absorption period (3s, 6s, 10s, 15s, 30s, and 1 minute) since the solution absorption rate is not constant. After taking the specimen out of solution, the surface moisture of specimen was removed rapidly with paper towel and put on the scale to measure its weight immediately. To eliminate the effect of moisture evaporation, the whole measurement process took less than 30 seconds. Since the sample was in meso-scale, though the evaporated water amount was small, it may be sensitive to the initial absorption results. When the absorption period was more than one minute, the specimen was put into solution with settled position by spacer. The measurement would continue with the steps described above except the interval time changes with the absorption period to 2, 3, 5, 10, 15, 20, 30, 40, 60 minutes, 8 hours and 1,2,3 days. In total, nine specimens (three of each for three different w/c) were tested in one container. The volume ratio of solution to samples was controlled over 40:1 as shown in Fig. 2(b).

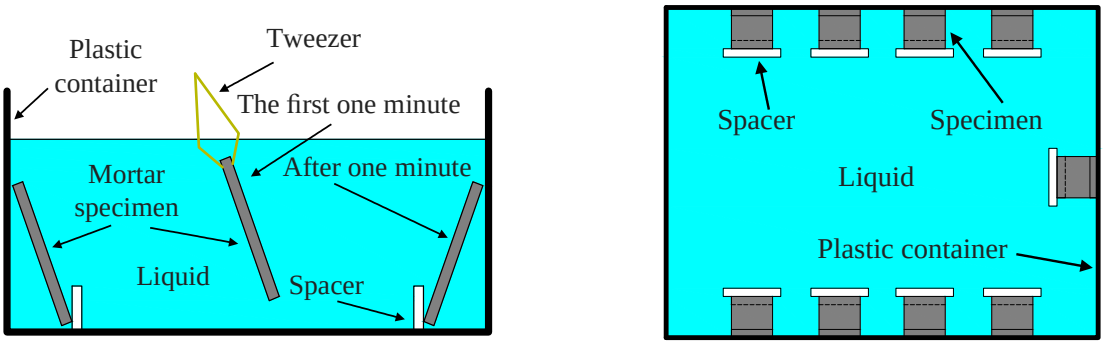

(a) side view (b) top view

Fig. 2 – Absorption test setup

After three days of absorption, the specimens were surface-dried by paper towel, and again put into oven for 24 hours at 105°C for drying. When they were taken out of oven, again, the saran was used to prevent moisture transfer. Once the specimen's temperature decreased to normal temperature, the dry weight of dried specimens was measured again. As a result, the mass change of dry weight and water loss during drying was obtained. Containers of deionized water were prepared for reabsorption. Regardless of DI water or NaCl solutions absorbed in the first stage, all the specimens were put into DI water for reabsorption. In this case, the difference in pore size distribution due to crystallization could be compared. Considering the possibility of ionic exchange during the reabsorption, the process was prolonged to seven days to observe the moisture transfer equilibrium.

3. Theoretical background

3.1 Two-stage absorption model

For one-dimensional liquid absorption, typically, the sorptivity of the sample can be obtained by fitting the following equation [12]:

$$\frac{W}{A} = St^{1/2} + S_0 = C\left(1-\exp\left(-St^{1/2}/C\right)\right) + S_{g0}t^{1/2} + S_0 \quad (1)$$

where W is the volume of water absorbed, A is the cross-sectional area of the water exposed surface, C is the constant related to the distance of initial sorption, S_{g0} is the coefficient for the relaxation effect, S is the sorptivity and S_0 is the constant for initial water content.

For the long time absorption, the water absorption is dominated by the $S_{g0}t^{1/2}$ term [12]. The relaxation effect means that, after bulk water absorption, the air voids in small pores flow out and the pore characteristics may be changed due to Ca^{2+} leaching and salt crystallization, which may promote further water ingress. However, these phenomena can also occur during the bulk water absorption, and they are related to the degree of saturation. Therefore, to have more accurate prediction, the coefficient of relaxation effect should be modified to consider the bulk water absorption, as below.

$$S_g = \frac{S_{g0}}{C\left(1-\exp\left(-St^{1/2}/C\right)\right)} \quad (2)$$

However, for three-dimensional liquid absorption, the model is supposed to be modified based on the water absorption capacity to consider the size of samples and it may be determined by the dried mass of the sample as follows:

$$q = \frac{m-m_d}{m_d} \quad (3)$$

where m is the mass of specimen having absorbed solution and m_d is the mass of dried specimen.

In three dimensions, the liquid exposed area could be considered as the exposed sample volume. If the sample is initially dried, the constant for initial water content S_0 is equal to zero. So Eq. (1) can be transformed to Eq. (4).

$$\frac{W}{V} = \frac{(m-m_d)\cdot\rho_b}{m_d\cdot\rho_l} = \frac{C}{h}\left(1+S_g t^{1/2}\right)\left(1-\exp\left(-St^{1/2}/C\right)\right) \quad (4)$$

where V is the apparent volume of the sample (the volume including the pore voids), ρ_l is the density of solution, ρ_b is the bulk dry density of sample S_g is the modified coefficient for relaxation effect and h is the thickness of the sample.

Combing Eqs. (3) and (4) yields Eq. (5).

$$q = \frac{C \cdot \rho_l}{h \cdot \rho_b}\left(1 + S_g t^{1/2}\right)\left(1 - \exp\left(-St^{1/2} / C\right)\right) \tag{5}$$

Besides, a more general parameter to evaluate the moisture transport is the apparent moisture diffusivity D_0, which can be estimated based on normalized sorptivity s [18].

$$D_0 = s^2 / 123.131 \tag{6}$$

$$s = \frac{S m_d \rho_l}{\left(m_{sat} - m_d\right)\rho_b} \tag{7}$$

$$S = \frac{11.1\left(m_{sat} - m_d\right)\rho_b \sqrt{D_0}}{m_d \rho_l} \tag{8}$$

where m_{sat} is the mass of saturated sample.

After the initial sorption, the capillary pores are fully filled by solution. The sample is in a quasi-equilibrium condition, in which almost all the pores are occupied by liquid except small pores filled by air, so that the sample is very close to full saturation and the liquid absorption rate becomes almost zero at that condition. It is reasonable to define the quasi-equilibrium solution uptake as follows:

$$q_\infty = \left(m'_{sat} - m_d\right) / m_d = C\rho_l / h / \rho_b \tag{9}$$

where m'_{sat} is the mass of quasi-saturated sample.

Therefore, the solution uptake could be described with the following two-stage model.

$$q = q_\infty \left(1 + S_g t^{1/2}\right) \left(1 - \exp\left(-11.1\left(\frac{D_0 t}{h^2}\right)^{1/2}\right)\right) \tag{10}$$

However, for different concentration solution, the solution mass gain may not show the transport characteristics very clearly. It is more realistic to normalize the solution uptake amount as Eq. (11).

$$Q = \frac{q\rho_b}{\rho_l} = \frac{\left(m - m_d\right)\rho_b}{m_d \rho_l} = \frac{V_l}{V} \tag{11}$$

where Q is the volume ratio of liquid volume to apparent volume of sample and V_l is the volume of liquid.

3.2 Relative sorptivity

Liquid absorption in mortar is mainly depending on liquid properties and pore structures. If the liquid properties change with solution concentration and temperature is known, the analysis of pore structure can be achieved based on the liquid absorption phenomenon.

For NaCl solution, three properties which may affect the solution absorption are surface tension, viscosity, and density. Besides, all of them are sensitive to the solution concentration and temperature. Therefore, the relationships between the three solution properties and coupled concentration and temperature effect are supposed to be developed. Then the solution absorption with different concentration solutions and temperatures can be clarified and the salt crystallization can also be analyzed.

Surface tension of NaCl solution has been studied by Villani et al. [22]. By regressing the experimental results, they fitted the parameters of a semiempirical formulation proposed by Szyszkowski to calculate the surface tension with temperature and concentration as Eq. (12) [22]:

$$\gamma = \gamma_{water,T} - RT\Gamma^\infty \ln\left(1 + \frac{c}{b}\right) \tag{12}$$

where Γ^∞=-3.86×10^{-6}mol/m^2, b=16.11%, γ is the surface tension of solution at temperature T, $\gamma_{water,T}$ is the surface tension of water at the same temperature T of the solution and c is the concentration of solution (% by mass). At 25°C, the surface tension of water is 71.97 mN/m [23].

In the above equation, the effect of temperature on the surface tension of water is still not clear. The relationship between surface tension of water and temperature can be as Eötvös rule [24].

$$\gamma_{water,T} = k\left(T_c - T\right) \tag{13}$$

where k is a constant (about 0.2056 mN/m/°C), T_c is the critical temperature of the surface tension of water/air reaching a value of 0 (T_c=374°C).

Substituting Eq. (13) into Eq. (12), the surface tension could be a function of temperature and

solution concentration as Eq. (14) and the predicted results of different temperatures are shown in Fig. 3(a).

$$\gamma = k\left(T_c - T\right) - RT\Gamma^{\infty} \ln\left(1 + \frac{c}{b}\right) \tag{14}$$

For the viscosity at normal temperature, Villani et al. (2014) also conducted test and predicted it based on the equation proposed by Kaminsky as below [22]:

$$\eta = \eta_{water}\left(1 + a_1 c^{1/2} + a_2 c + a_3 c^2\right) \tag{15}$$

where η is the viscosity of NaCl solution at a certain temperature and pressure, η_{water} is the viscosity of pure water at the same temperature and pressure, a_1, a_2 and a_3 are constants determined by fitting the test results and a_1=0.1134, a_2=-0.0551, a_3= 0.0027.

The temperature effect on viscosity can be described with Arrhenius type of law as Eq. (16).

$$\eta = A \cdot \exp\left(\frac{E_a}{R_g T}\right) \tag{16}$$

From the test results of Villani et al. [22], E_a is the activation energy which is around 20.9kJ/mol for NaCl solution. R_g is the universal gas constant (8.314 J/K/mol), and the parameter A is a constant changing with concentration of NaCl. For the same concentration solution, the viscosity may be predicted based on the viscosity at reference temperature from Eq. (17):

$$\eta = \eta_0 \exp\left[\frac{E_a}{R_g}\left(\frac{1}{T} - \frac{1}{T_0}\right)\right] \tag{17}$$

where η_0 is the viscosity at reference temperature T_0.

Therefore, the viscosity of salt solutions with temperature and concentration change can be derived as follows:

$$\eta = \eta_{water,T_0} \cdot \left(1 + a_1 c^{1/2} + a_2 c + a_3 c^2\right) \cdot \exp\left[\frac{E_a}{R_g}\left(\frac{1}{T} - \frac{1}{T_0}\right)\right] \tag{18}$$

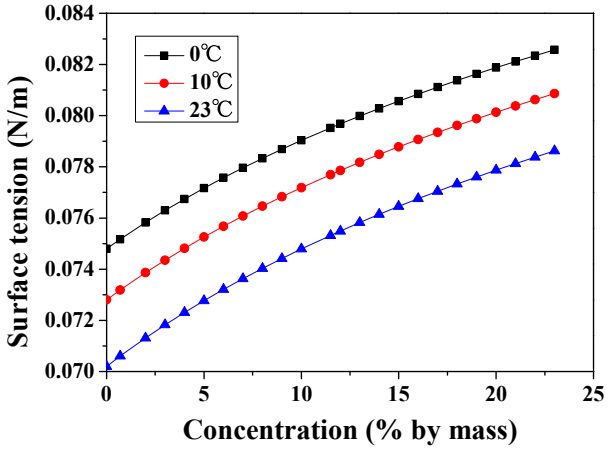

(a) Surface tension

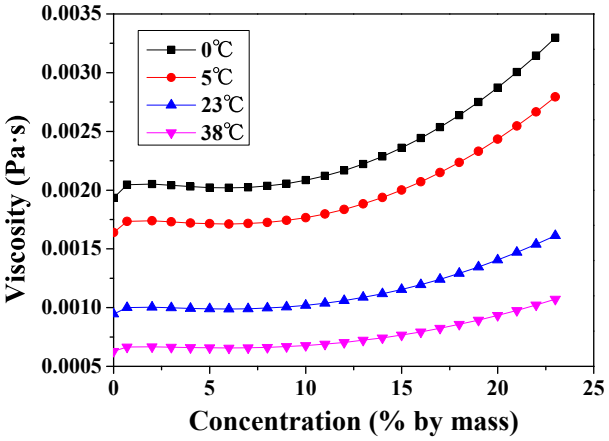

(b) Viscosity

Fig. 3 – Influence of temperature on NaCl solution properties

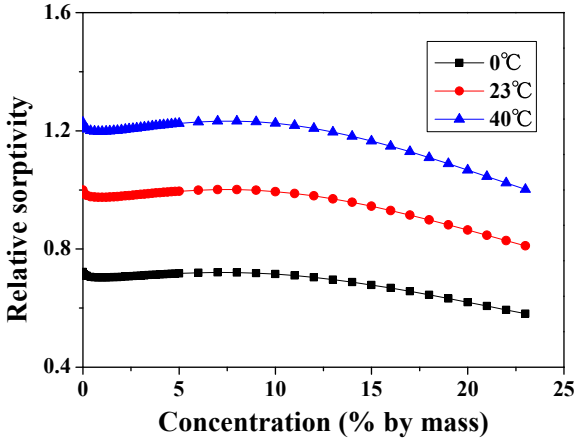

Fig. 4 – Relative sorptivity change with solution concentration

where $\eta_{water,T0}$ is the viscosity of pure water at the reference temperature. From Wikipedia [25], at 25°C, the viscosity of water is 8.94×10^{-4} Pa·s. Based on Eq. (18), the viscosity is predicted as shown in Fig. 3(b).

The density of NaCl solution at 23 °C is calculated as Eq. (19) [26].

$$\rho_l = 7.2011c + 997.83 \quad (19)$$

Following Hall and Hoff [27], if samples share the same pore structure, then the solution absorption would vary with the ratio of surface tension and viscosity. So the relative sorptivity can be defined as γ/η, which is shown in Fig. 4. The relative sorptivity changes with temperature and concentration and it may reach the maximum value at intermediate concentration (3% to 10% by mass).

4. Results and discussions

4.1 Absorbed water content during the first absorption

After 3 days immersion into solutions, the water absorbed was measured by gravimetrical method. Theoretically, if there is no Ca^{2+} leaching and salt crystallization, the absorbed water content can be calculated based on total amount of absorbed solution and the concentration of pore solution. The total amount of absorbed solution can be known with the difference between the mass at full saturation and initial dried samples. Since the sample size is in meso scale in this study, the concentration of pore solution can be considered as the same with surrounding environment (solution concentration to which the sample was exposed). Therefore, the absorbed water amount could be normalized to the dried mass of sample as Eq. (3), and the normalized absorbed water will be as follows:

$$m_w = q_{\max} \cdot (1 - c) \quad (20)$$

where q_{max} is the maximum normalized solution uptake.

Due to the possible Ca^{2+} leaching, the absorbed water content is not equal to the difference between the initial dried sample mass and saturated sample mass. Instead, it is more reasonable to calculate the absorbed water based on the difference between the re-dried sample mass and the saturated sample mass, considering the water absorption capacity difference, it can be normalized as below:

$$m_w = \frac{m_{sat} - m_{dre}}{m_d} \quad (21)$$

where m_{dre} is the re-dried mass of sample.

As shown in Fig. 5, samples exposed to DI water show that the absorbed water amount calculated by Eq. (21) is higher than the amount by Eq. (20), which means part of mortar matrix was replaced by water due to Ca^{2+} leaching. Clearly, samples exposed to 3% NaCl solution also show the tendency, in this case, the matrix mass change is dominated by Ca^{2+} leaching although it is co-existing with salt crystallization. However, samples exposed to 20% NaCl solution show different tendency compared with the two cases mentioned above except the *w*/*c*=0.3 case. This can be explained by the filling of pores by crystallized salt since the amount of crystallized salt increases with the increase of concentration of solution. However, due to the less porous media in samples with

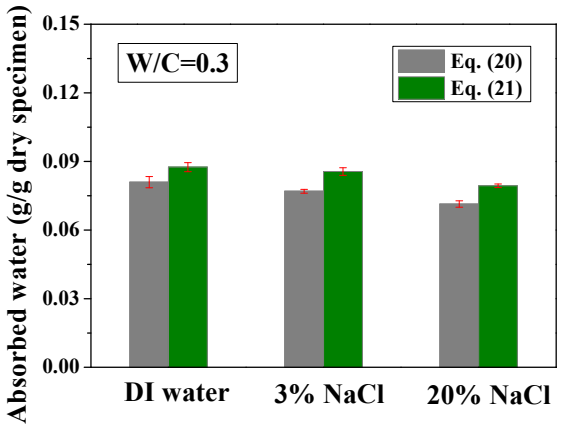

(a) 0.3

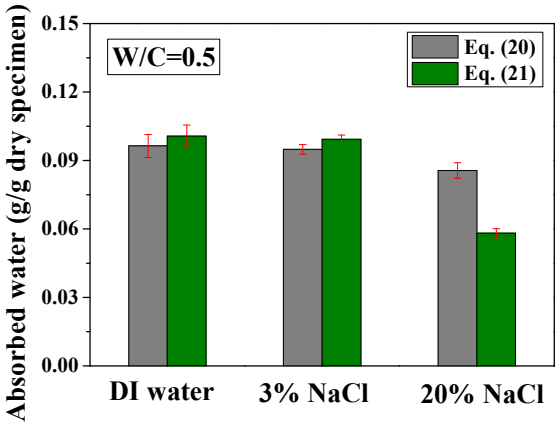

(b) 0.5

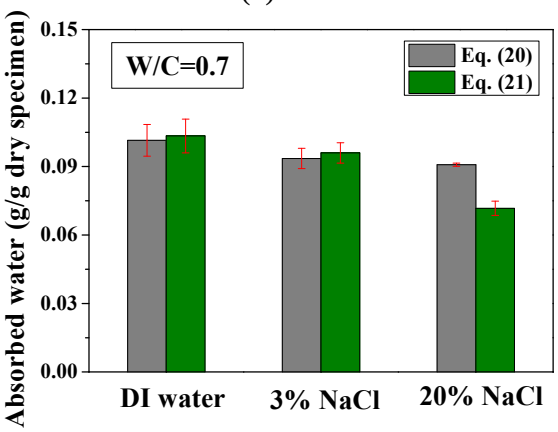

(c) 0.7

Fig. 5 – Normalized absorbed water content with different *w*/*c*

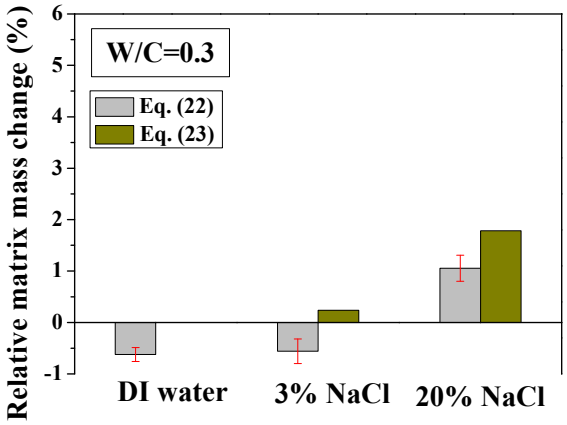

(a) 0.3

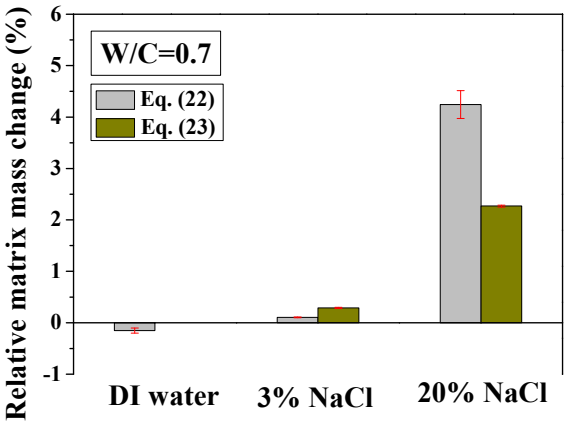

(b) 0.5

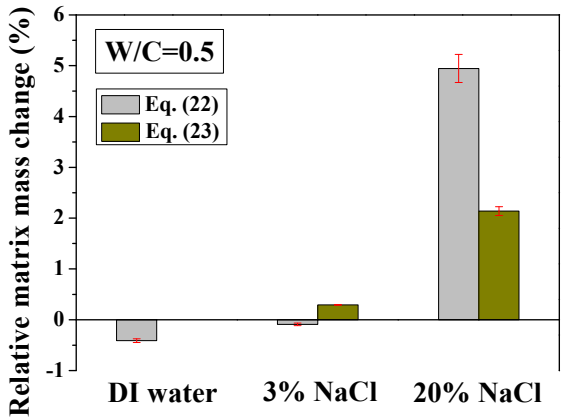

(c) 0.7

Fig. 6 – Mass change of mortar before absorption and oven dried after absorption with different *w*/*c*

w/*c*=0.3, the specific surface area is limited for salt crystallization to occur. As a result, the effect of salt crystallization cannot compensate the effect of leaching in the case of *w*/*c*=0.3. Also, it is interesting to note that the actual absorbed water content in samples exposed to high concentration solution is much lower than the one absorbed from DI water, which means that samples saturated with higher concentration solution may suffer from smaller internal stress induced by ice expansion. However, for intermediate concentration case (3% NaCl), in terms of absorbed water amount, there is no big difference compared with DI water. If the temperature decreases to subzero, the water would form ice and the expansion could induce internal pressures to cause micro cracks and then macro cracks. At low temperature, the solubility of calcium hydroxide would be higher than at normal temperature since it increases with decreasing temperature. In this case, NaCl may react with the calcium hydroxide to form Friedel's salt. Because of the expansion of Friedel' salt, additional pressures will be induced. Therefore, the internal pressure due to the combined ice formation and salt crystallization during freezing is more severe than the pressure induced by ice formation alone in the case of DI water. This may imply the reason why the most destructive damage happens at the intermediate concentration case.

4.2 Mass change of mortar matrix after solution absorption

After the sample was exposed to solution, the mass of mortar matrix may be changed. In the case of DI water, the only possible mass change besides water uptake is the leaching of calcium hydroxide. However, for NaCl contaminated samples, in addition to the reduced mass due to leaching, the formation of salt and precipitation of NaCl can gain the mass. Since the mass increase contributed by NaCl precipitation is known, the proportion from crystallization can be estimated.

The amount of mass change can be calculated based on the difference between the initial dried mass and re-dried mass, considering the water absorption capacity difference, and it can be normalized as below.

$$\Delta m = \frac{m_{dre} - m_d}{m_d} \tag{22}$$

In addition, if there is no leaching or salt crystallization, the mass change is due to the precipitation of NaCl. Since the concentration of pore solution is known, the amount of mass gain can be estimated as Eq. (23).

$$\Delta m_{NaCl} = \frac{\left(m_{sat} - m_d\right) \cdot c}{m_d} \tag{23}$$

As shown in Fig. 6, the matrix mass loss was observed in case of DI water, and the amount reduces with increasing *w*/*c*. This phenomenon is corresponding to the amount of absorbed water and the reason is due to Ca^{2+} leaching as explained in section 4.1. With increasing solution concentration, the mass change increases gradually. It seems that the mass change tendency of the 3% NaCl case is from negative to positive with increasing *w*/*c*,

which may indicate that the amount of crystallized salt is increasing with the porosity. More importantly, for the case of 20% NaCl, the mass change value from Eq. (22) is higher than the value from Eq. (23) for the case of *w*/*c*=0.5 and 0.7. It proves that there is formation of new salts (eg. Friedel's salt), which increased the matrix mass of sample in addition to NaCl precipitation. The difference between the two results could be contributed to the newly formed salt (eg. Friedel's salt), and it is found that the amount of the salt is even higher than the precipitation of NaCl. In addition, it is worth noting that, for the case of *w*/*c*=0.3, the different tendency was observed. This implies that even under high concentration, the Ca^{2+} leaching phenomenon is still happening. Therefore, the actual crystalized salt amount is greater than the estimation and this amount of salt may have expansion enough to cause damage in the mortar specimen.

4.3 Solution absorption and water reabsorption of sample

For a short period of immersion (1 hour), the test results of cumulative solution absorption characteristics are presented in Figs. 7 through 10 with the square root of time. While for a longer period (7 days), as shown in Fig. 11, the absorption results are presented with the exponent of time. The absorption amount is analyzed based on Eq. (3), normalized by the dried mass of sample. As found in Fig. 7(a), the absorption process may be divided into two stages, initial absorption and long time absorption. The differences among the two stages are more obvious in Fig. 11. During the initial absorption, the mass of sample increased linearly and rapidly. This may be contributed by the capillary pore absorption. If the pores can be assumed to be continuous tubes for solution transport, the larger diameter can transport the solution more speedily [11-13]. For the long time absorption, it is also linear (see Fig. 11). The gel pore solution absorption and filling of air voids may be responsible for mass gain during this period. Due to the small size of gel pores, the solution transport inside could be rather slow, so it needs a long time to be totally filled by water. In macro scale test in a past study [17], only the above two processes are obvious and it is a knee point that separates them. However, in meso-scale absorption test, there is no clear knee point, instead, a transition region in an exponential relationship with time was observed, which is clearly shown in Figs. 7 through 10.

In Figures 7 through 9, the solution absorption is related to solution mass gain. Due to the solution

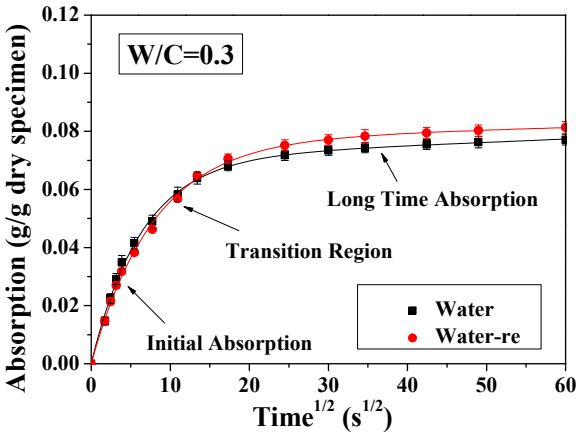

(a) *w*/*c* = 0.3

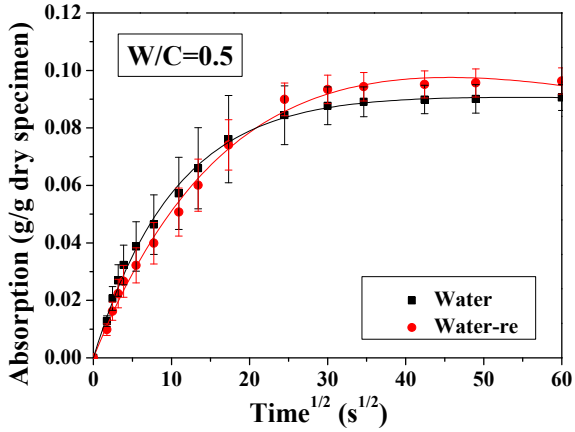

(b) *w*/*c* = 0.5

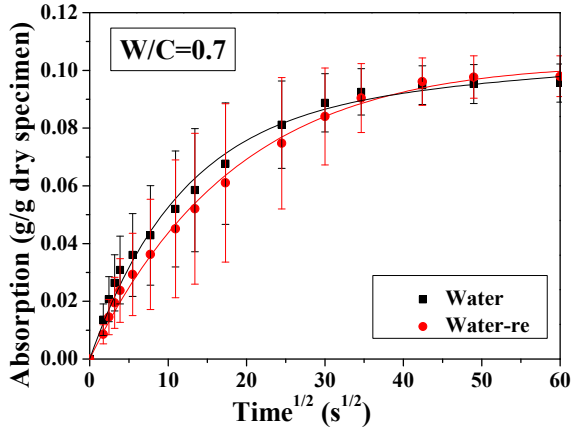

(c) *w*/*c* = 0.7

Fig.7 – Comparison of water absorption and water reabsorption mass in mortar within 60 minutes

density difference, the absorption amount in terms of volume for each concentration solution cannot be seen. In order to see the concentration effect, the absorbed solution volume to sample volume ratio, which was calculated based on Eq. (11), was compared among different concentration cases in Fig. 10. For different *w*/*c*, the absorption results are different. In case of 20% NaCl solution, samples with *w*/*c*=0.3 has the lowest absorbed solution volume while it is increasing with *w*/*c* and becoming the highest for the sample with *w*/*c*=0.7.

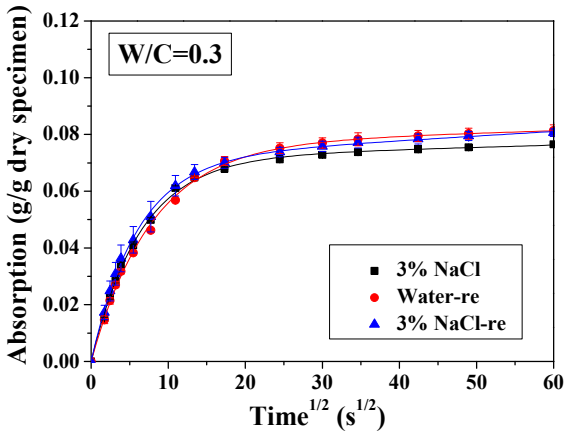

(a) w/c = 0.3

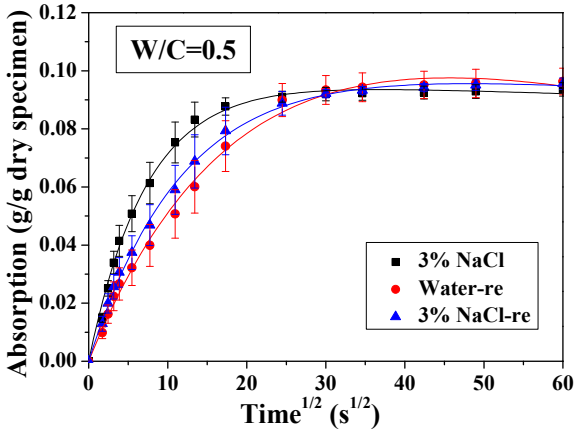

(b) w/c = 0.5

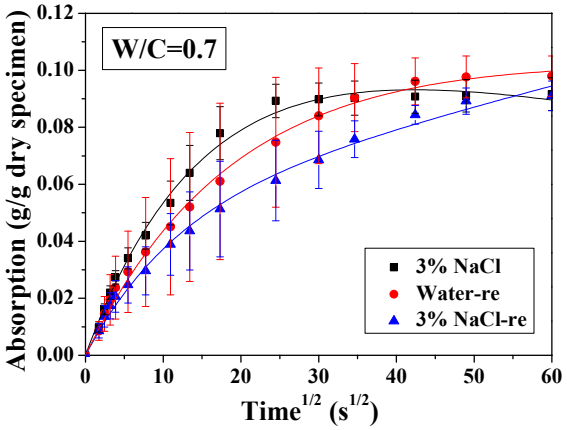

(c) w/c = 0.7

Fig. 8 – Comparison of 3% NaCl solution absorption and water reabsorption mass in mortar within 60 minutes

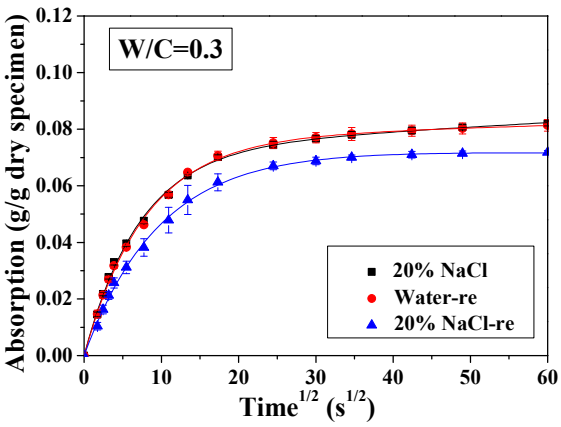

(a) w/c = 0.3

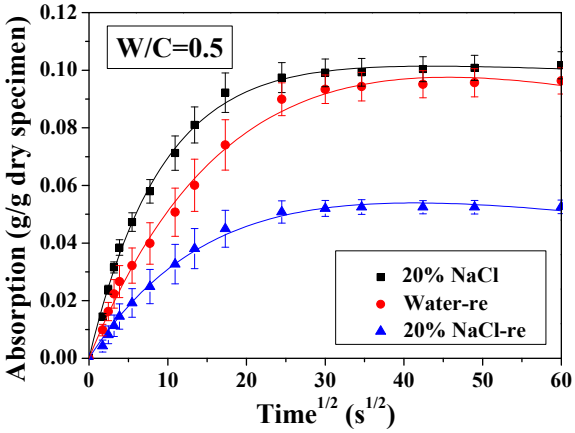

(b) w/c = 0.5

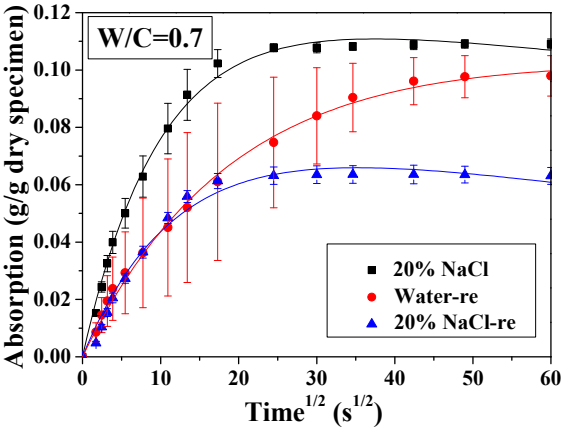

(c) w/c = 0.7

Fig. 9 – Comparison of 20% NaCl solution absorption and water reabsorption mass in mortar within 60 minutes

The two-stage absorption model, which is shown by solid lines in Figs. 7 through 10, fit well the absorption processes of mortar samples (w/c=0.3, 0.5, and 0.7) in 0, 3%, and 20% NaCl solutions and reabsorption processes in DI water. The parameters q_∞, Q_∞, D_0 and S_g are summarized in Table 3. Compared with water absorption and water reabsorption curves in Fig. 7, the slope during initial absorption becomes smaller in the reabsorption process, but the cumulative absorption amount exceeds the initial absorption at long time absorption period. Besides, in all 3% NaCl solution cases, parameters D_0 and S_g decreased during reabsorption while the parameters q_∞ and Q_∞ increased. This trend implies that the volume of capillary pores is reduced because the solution can be transported faster in capillary pores compared with in gel pores as aforementioned. The total pore volume is increased since the maximum absorption amount, which is determined by the total pore

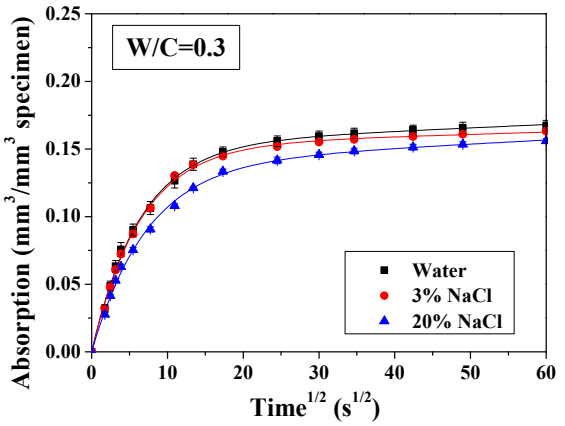

(a) *w*/*c* = 0.3

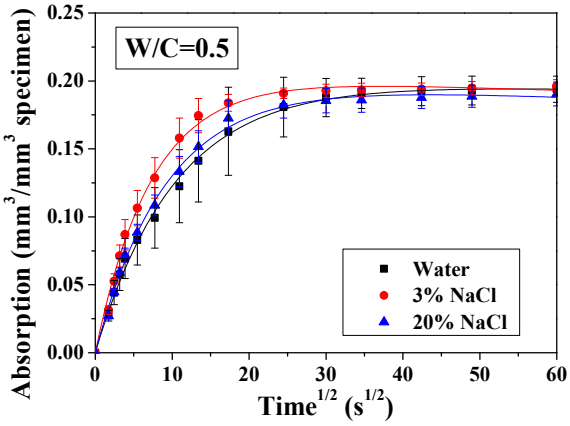

(b) *w*/*c* = 0.5

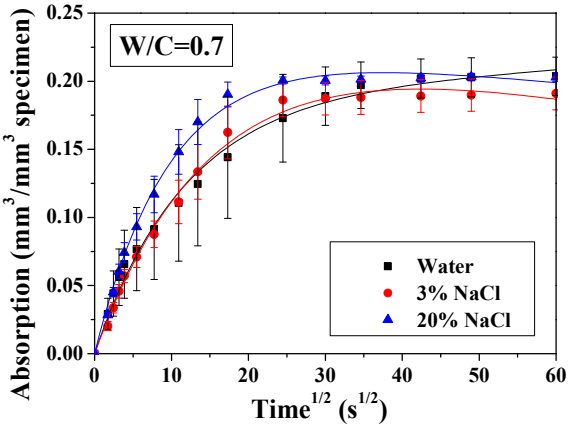

(c) *w*/*c* = 0.7

Fig. 10 – Comparison of absorbed solution volume to sample volume ratio in mortar within 60 minutes with solid lines representing the curve fitting by the two-stage model

volume, is increased. The reduction of capillary pores may be caused by salt crystallization and the thermal shrinkage due to oven drying, whilst the increasing porosity may be caused by the Ca^{2+} leaching and it mainly affects the gel pores.

In case of 20% NaCl solution exposed samples, the reabsorption curves are very different from the samples exposed to DI water, especially for higher porosity samples. Besides, as shown in Table 3, the fitted parameter of quasi-equilibrium solution uptake and relaxation parameter of 20% NaCl solution exposed samples are smaller while the apparent diffusion coefficient is higher except the case of *w*/*c*=0.3. Interestingly, for 3% NaCl solution, both of the apparent diffusion coefficient and relaxation parameter are the highest compared with other two solution cases. This is because the precipitated salt is insignificant to porosity alteration for the low concentration one and also the effect of leaching may compensate the effect of precipitated salt. However, the porosity is dramatically reduced for high concentration NaCl solution immersed samples, which means the leaching effect will not increase with solution concentration but the salt crystallization effect will. In addition, the porosity alteration is increasing with *w*/*c*. This is due to the possibility that more porous microstructural characteristics can promote the salt crystallization.

5. Conclusions

Based on the proposed two-stage NaCl solution diffusion model, experimental results of mortar solutions absorption and water reabsorption can be described well. The following conclusions can be reached.

(1) The solution transport depends on the pore characteristics of mortar. As a result, it varies with different *w*/*c*. The solution property change with solution concentration and temperature are analyzed and the relative sorptivity change with concentration is presented. The overall transport behavior difference with solute difference at 23°C can be explained by the difference in two phenomena, salt crystallization and Ca^{2+} leaching.

(2) Exposure to intermediate concentration (3% by weight) solution, although the salt crystallization and Ca^{2+} leaching were co-existing, the sample absorbed almost the same amount of water as DI water case. When ice formation and salt crystallization occur at subzero temperature, the expansion due to ice and salt induce internal pressures. The pressure is more severe than the pressure in the DI water case, which is induced by ice formation alone, resulting in more destructive frost damage.

(3) Exposure to high concentration (20% by weight) solution, the salt crystallization has greater effect on transport properties of mortar than Ca^{2+} leaching. The salt fills the voids or blocks the gel pores with solution transport.

Table 3 – The fitted parameters during NaCl solution absorption or water reabsorption

	Absorption (w/c=0.3)				Reabsorption (w/c=0.3)			
Immersed solution	q_∞ (%)	Q_∞ (%)	D_0 ($\times10^{-3}$mm^2/s)	S_g ($\times10^{-3}$s$^{1/2}$)	q_∞ (%)	Q_∞ (%)	D_0 ($\times10^{-3}$mm^2/s)	S_g ($\times10^{-3}$s$^{1/2}$)
DI water	0.071	0.153	5.09	1.6	0.077	0.166	3.35	1.05
3% NaCl	0.072	0.153	4.93	1.09	0.071	0.155	5.71	2.26
20% NaCl	0.073	0.139	3.91	2.12	0.073	0.159	2.08	-0.31
	Absorption (w/c=0.5)				Reabsorption (w/c=0.5)			
Immersed solution	q_∞ (%)	Q_∞ (%)	D_0 ($\times10^{-3}$mm^2/s)	S_g ($\times10^{-3}$s$^{1/2}$)	q_∞ (%)	Q_∞ (%)	D_0 ($\times10^{-3}$mm^2/s)	S_g ($\times10^{-3}$s$^{1/2}$)
DI water	0.094	0.201	2.48	-0.52	0.139	0.298	0.65	-4.67
3% NaCl	0.097	0.204	4.86	-0.90	0.105	0.225	1.82	-1.48
20% NaCl	0.107	0.200	3.2	-0.99	0.074	0.158	0.94	-4.7
	Absorption (w/c=0.7)				Reabsorption (w/c=0.7)			
Immersed solution	q_∞ (%)	Q_∞ (%)	D_0 ($\times10^{-3}$mm^2/s)	S_g ($\times10^{-3}$s$^{1/2}$)	q_∞ (%)	Q_∞ (%)	D_0 ($\times10^{-3}$mm^2/s)	S_g ($\times10^{-3}$s$^{1/2}$)
DI water	0.088	0.187	1.59	1.96	0.109	0.231	0.55	-0.65
3% NaCl	0.121	0.254	0.89	-4.1	0.052	0.112	2.32	13.47
20% NaCl	0.125	0.232	1.77	-2.33	0.082	0.175	1.2	-4.26

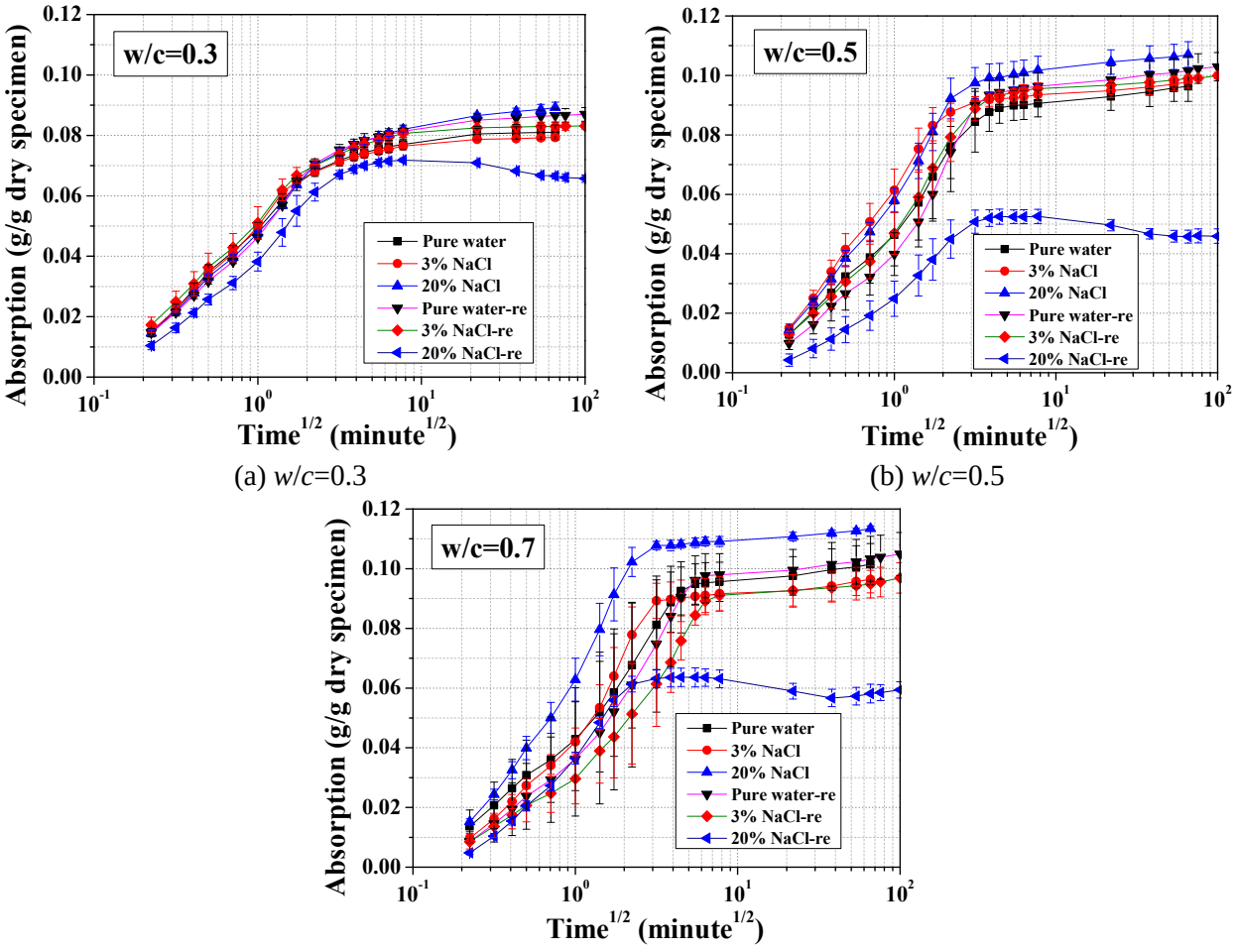

(a) w/c=0.3 (b) w/c=0.5

(c) w/c=0.7

Fig. 11 – Comparison of solution absorption and water reabsorption mass in mortar within 7 days

Subsequently, it reduced the further water penetration, so that the specimen would have less degree of expansion when the water transforms to ice.

(4) The rate of absorption in each stage is related to the pore diameters of mortar. By developing the model connected with pore diameter and absorption, the pore diameter change in each range may be understood accurately. This will be reported in the future study.

Acknowledgements

The authors would like to express their sincere thanks to the Grant-in-Aid for Scientific Research (A) of Japan Society of Promotion of Science (No. 26249064) and the research fund of Ministry of Transport Construction Technology of China (No. 2014318494020). The first author would also like to show his gratitude to the scholarship granted by Chinese Scholarship Council (CSC) which supports the author's PhD study and research work.

References

1. Valenza II, J. J. and Scherer, G. W. (2007) "A review of salt scaling: II. Mechanisms," Cement and Concrete Research, 37, pp. 1022-1034.
2. Fagerlund, G. (1996) "Predicting the service life of concrete exposed to frost action through a modeling of the water absorption process in the air-pore system," Springer.
3. Yang, Z.; Weiss, W. J.; and Olek, J. (2006) "Water transport in concrete damaged by tensile loading and freeze–thaw cycling." Journal of materials in civil engineering, 18(3), pp. 424-434.
4. Hashimoto, K. and Yokota, H. (2013) "Pore Structure Analysis of Mortar under Freeze-Thaw Cycles Using Mercury Intrusion Porosimeter," Journal of the Society of Materials Science, Japan, 62(8), pp. 486-491. (*In Japanese*)
5. Farnam, Y.; Washington, T.; and Weiss, J. (2015) "The Influence of Calcium Chloride Salt Solution on the Transport Properties of Cementitious Materials," Advances in Civil Engineering, 2015, pp. 1-13.
6. Baroghel-Bouny, V.; Wang, X.; Thiery, M.; Saillio, M.; and Barberon, F. (2012) "Prediction of chloride binding isotherms of cementitious materials by analytical model or numerical inverse analysis," Cement and Concrete Research, 42, pp. 1207-1224.
7. Florea, M. and Brouwers, H. (2012) "Chloride binding related to hydration products: Part I: Ordinary Portland cement," Cement and Concrete Research, 42(2), pp. 282-290.
8. Valenza II, J. J. and Scherer, G. W. (2005) "Mechanisms of salt scaling," Materials and Structures, 38, pp. 479-488.
9. Liu, J.; Tang, K.; Qiu, Q.; Pan, D.; Lei, Z.; and Xing, F. (2014) "Experimental Investigation on Pore Structure Characterization of Concrete Exposed to Water and Chlorides," Materials, 7(9), pp. 6646-6659.
10. Sato, Y.; Miura, T.; and Nakamura, H. (2015) "Meso-Scale Analysis of the Mechanical Properties of Chemically-Deteriorated Mortar," Proceedings of the 10th International Conference on Mechanics and Physics of Creep, Shrinkage, and Durability of Concrete and Concrete Structures, Vienna, Austria.
11. Kelham, S. (1988) "A water absorption test for concrete," Magazine of Concrete Research, 40, pp. 106-110.
12. Martys, N. S. and Ferraris, C. F. (1997) "Capillary transport in mortars and concrete," Cement and Concrete Research, 27, pp. 747-760.
13. Liu, Z. and Hansen, W. (2015) "Pore damage in cementitious binders caused by deicer salt frost exposure," Construction and Building Materials, 98, pp. 204-216.
14. Hall, C. and Tse, T. K. M. (1986) "Water movement in porous building materials—VII. The sorptivity of mortars," Building and Environment, 21, pp. 113-118.
15. Wang, L. and Ueda, T. (2011) "Mesoscale modeling of water penetration into concrete by capillary absorption," Ocean Engineering, 38, pp. 519-528.
16. Spragg, R. P.; Castro, J.; Li, W. T.; Pour-Ghaz, M.; Huang, P. T.; and Weiss, J. (2011) "Wetting and drying of concrete using aqueous solutions containing deicing salts," Cement Concrete Composites, 33, pp. 535-542.
17. Chandra, S. and Xu, A. (1992) "Influence of presaturation and freeze-thaw test conditions on length changes of portland cement mortar," Cement and Concrete Research, 22, pp. 515-524.
18. Wang, L. and Ueda, T. (2013) "Mesoscale Modeling of Chloride Penetration in Unsaturated Concrete Damaged by Freeze-Thaw Cycling," Journal of Materials in Civil Engineering, ASCE, 26, pp. 955-965.
19. Macinnis, C. and Nathawad, Y. (1980) "The effects of a deicing agent on the absorption and permeability of various concretes," ASTM special technical publication, 691, pp. 485-496.
20. ACI Committee 211 (1991) "Standard practice for selecting properties for normal, heavyweight, and mass concrete," American Concrete Institute, ACI 211.1-91, Detroit.
21. ASTM, C. 1585–04. (2004) "Standard Test Method for Measurement of Rate of Absorption of Water by Hydraulic-Cement Concretes," ASTM International.
22. Villani, C.; Spragg, R.; PourGhaz, M.; and Jason Weiss, W. (2014) "The Influence of Pore Solutions Properties on Drying in Cementitious Materials," Journal of the American Ceramic Society, 97(2), pp. 386-393.
23. https://en.wikipedia.org/wiki/Surface_tension
24. Adam, Neil Kensington (1941) "The Physics and Chemistry of Surfaces," 3rd ed., Oxford University Press.
25. https://en.wikipedia.org/wiki/Viscosity
26. Quanbing, Y. (2007) "Effects of sodium chloride concentration on saturation degree in concrete under freezing-thawing cycles," Journal of the Chinese Ceramic Society, 1, pp. 96-100. (*In Chinese*)

27. Hall, C. and Hoff, W. (2002) "Water transport in brick, stone and concrete," Spon Press, London.